Failure of a Two-State Model To Describe the Influence of Phospho(*enol*)pyruvate on Phosphofructokinase from *Escherichia coli*†

Jason L. Johnson‡ and Gregory D. Reinhart*,§

Department of Chemistry, Southwestern Oklahoma State University, Weatherford, Oklahoma 73096, and Department of Biochemistry and Biophysics, Texas A&M University, College Station, Texas 77843-2128

Received April 23, 1997; Revised Manuscript Received August 7, 1997⊗

ABSTRACT: A linked-function analysis is presented of the influence of the inhibitor phospho(*enol*)pyruvate (PEP) on the binding of fructose 6-phosphate (Fru-6-P) and MgATP to phosphofructokinase (PFK) from *Escherichia coli*. The results of this analysis indicate that the previously described inhibition of Fru-6-P binding by MgATP [Johnson, J. L., & Reinhart, G. D. (1992) *Biochemistry 31*, 11510−11518] is almost completely independent of the inhibition by PEP. Moreover, with or without the presence of MgATP, the inhibition by PEP does not conform to the behavior expected if PEP and Fru-6-P bind exclusively to different enzyme forms since the formation of a ternary complex with both PEP and Fru-6-P bound is clearly evident at high concentrations of Fru-6-P and PEP. van't Hoff analyses of the coupling interactions between PEP and Fru-6-P in the presence and absence of MgATP indicate that these couplings are driven by enthalpy. However, the influence that PEP has on MgATP binding is small and changes from being activating to being inhibitory at temperatures above 40 °C, revealing the importance of a compensating entropy component to the coupling interactions. The four functionally defined enzyme forms that contribute to the coupling between Fru-6-P and PEP were evaluated structurally using the fluorescence properties of the single intrinsic tryptophan as a probe. The steady-state and dynamic fluorescence emission and polarization properties of the tryptophan, as well as its susceptibility to I^- quenching, indicate that the flexibility of PFK in the vicinity of the tryptophan is perturbed by the binding of ligands. The properties of free PFK do not lie between those established by the binding of Fru-6-P and PEP individually, indicating that it is structurally distinct. The properties of the ternary complex lie between those of the singly-ligated forms. Though an equilibrium mixture of two conformations of ternary complex cannot therefore be formally ruled out, no evidence obtained to date requires the presumption of this mechanistic complication.

During the conversion of glucose to pyruvate, phosphofructokinase (PFK)[1] from *Escherichia coli* transfers a phosphate group from MgATP to fructose 6-phosphate (Fru-6-P), yielding the products MgADP and fructose 1,6-bisphosphate. PFK is subject to allosteric activation by MgADP and inhibition by phospho(*enol*)pyruvate (PEP) in that MgADP promotes, and PEP antagonizes, the affinity by which Fru-6-P binds to the enzyme. Yet both MgADP and PEP bind to the same site on the enzyme (Blangy et al., 1968). The actions of these effectors have traditionally been viewed within the constraints of the concerted two-state model (Monod et al., 1965; Rubin & Changeux, 1966; Blangy et al., 1968). According to this model, MgADP and PEP preferentially bind to R and T enzyme forms, respectively, shifting the equilibrium between the two enzyme conformations and thereby selectively increasing the population of R or T. Fru-6-P in turn is presumed to exhibit very high and very low affinity for the R and T states, respectively, and consequently its binding promotes a T → R transition.

Crystal structures detailing structural differences between Fru-6-P-bound and inhibitor-bound forms of PFK from *Bacillus stearothermophilus* (Evans & Hudson,1979; Evans et al., 1981; Schirmer & Evans, 1990) have served to reinforce the presumed validity of the two-state model such that it has even been accepted by leading biochemistry textbooks [e.g., Voet and Voet (1995)] as the operative mechanism that leads to the allosteric properties of PFK. Recent studies, however, have revealed deficiencies in this model (Johnson & Reinhart, 1992, 1994a,b; Zheng & Kemp, 1992). For example, MgADP and Fru-6-P cause different structural changes in PFK, clearly indicated by the fluorescence polarization exhibited by the single intrinsic tryptophan (Johnson & Reinhart, 1994a). Also, the two-state model cannot adequately explain the actions of MgATP since MgATP allosterically antagonizes the binding of both Fru-6-P and MgADP (Zheng & Kemp, 1992), yet both MgATP and Fru-6-P bind to free enzyme with high affinity (Johnson & Reinhart, 1992). Moreover, the actions of MgADP cannot simply be viewed in relation to its effects on the binding of Fru-6-P since MgADP bound to the effector site simultaneously antagonizes the binding of MgATP, the other substrate of the enzyme.

† Much of the research reported herein was performed while the authors were members of the Department of Chemistry and Biochemistry at the University of Oklahoma, Norman, OK 73019. This work was supported by National Institutes of Health Grant GM 33216 and HRO-025 from the Oklahoma Center for the Advancement of Science and Technology.

* Author to whom correspondence should be addressed. E-mail: gdr@tamu.edu.

‡ Southwestern Oklahoma State University.

§ Texas A&M University.

⊗ Abstract published in *Advance ACS Abstracts,* October 1, 1997.

[1] Abbreviations: PFK, phosphofructokinase; Fru-6-P, fructose 6-phosphate; PEP, phospho(*enol*)pyruvate; MOPS, 3-(*N*-morpholino)propanesulfonic acid; EPPS, *N*-(2-hydroxyethyl)piperazine-*N*′-(3-propanesulfonic acid); BCA, bicinchoninic acid; DTT, dithiothreitol.

S0006-2960(97)00942-2 CCC: $14.00 © 1997 American Chemical Society

It is, however, the contrast between the actions of MgADP and PEP that provides the primary impetus to the two-state view in general, and we therefore present in this report a thorough linked-function analysis of the antagonism between Fru-6-P and PEP, including a consideration of their individual and combined interactions with MgATP. van't Hoff analyses of these coupling interactions have been performed to further characterize the thermodynamic forces that govern net allosteric response, with particular attention given to the contribution by entropy to coupling free energy (Reinhart et al., 1989). The sign of this entropy term has previously been correlated with the dynamic attributes of the single tryptophan per subunit in each of the enzyme forms relevant to MgADP inhibition of MgATP binding and activation of Fru-6-P binding (Johnson & Reinhart, 1994b). Similarly, perturbations deriving from the binding of Fru-6-P and PEP, both individually and in combination, are examined here using steady-state and dynamic fluorescence techniques on PFK's intrinsic tryptophan (Trp 311). Notably, a description of the ternary complex of Fru-6-P and PEP with PFK, a form usually not considered by the two-state model, proves to be necessary for understanding the nature of the inhibition produced by PEP. In addition, MgATP's role once again cannot be adequately explained within the constraints imposed by a two-state model.

MATERIALS AND METHODS

Materials. Phosphofructokinase was purified from *E. coli* K12, carrying the wild-type *pfkA* gene, obtained as a frozen paste from Grain Products Corp. All chemical reagents used in buffers, PFK purification, and fluorescence and enzymatic assays were of analytical grade, purchased from either Sigma, Fisher, or Aldrich. The Matrex Gel Blue A−agarose resin for affinity chromatography was purchased from Amicon Corp. Creatine phosphate, creatine kinase, the potassium salt of Fru-6-P, the sodium salts of PEP and ATP, and the coupling enzymes aldolase, triosephosphate isomerase, and glycerol-3-phosphate dehydrogenase in ammonium sulfate suspensions were obtained from Sigma. Coupling enzymes were dialyzed extensively against a buffer consisting of 50 mM MOPS-KOH, 100 mM KCl, 5 mM $MgCl_2$, and 100 μM EDTA at pH 7.0. Deionized distilled water was used throughout.

PFK Purification. PFK was purified via a modification of the method of Kotlarz and Buc (1982) as described previously (Johnson & Reinhart, 1992).

Enzyme Activity Determination. Activity measurements were carried out in 1.0 mL of an EPPS buffer adjusted to pH 8.0 at the appropriate temperature and containing 50 mM EPPS-KOH, 10 mM $MgCl_2$, 10 mM NH_4Cl, 0.1 mM EDTA, 2 mM DTT, 0.2 mM NADH, 250 μg of aldolase, 50 μg of glycerol-3-phosphate dehydrogenase, 5 μg of triosephosphate isomerase, 1 mM creatine phosphate, 10 μg/mL creatine kinase, and the indicated concentrations of Fru-6-P and MgATP. The enzymatic reaction was initiated with 10 μL of suitably diluted PFK. The steady-state reaction rate was determined by monitoring the decrease in absorbance at 340 nm with respect to time on a strip-chart recorder tracing after the disappearance of any slow, pre-steady-state transients. A unit of activity is designated as the amount of enzyme required to produce 1 μmol of fructose 1,6-bisphosphate/min.

Protein Determination. Protein concentrations were determined using the BCA protein assay reagent (Smith et al., 1985), which were complemented by absorbance readings [$\epsilon_{278} = 0.6$ cm^2 mg^{-1} (Kotlarz & Buc, 1977)] when nucleotides were not present.

Steady-State Fluorescence Measurements. Steady-state intensity and anisotropy of the intrinsic PFK fluorescence was measured on an ISS Model K2 multifrequency phase fluorometer. A xenon arc lamp provided the excitation source for intensity measurements, while the 300-nm line of a Spectra-Physics Model 2045 argon ion laser was used in anisotropy measurements. The excitation beam from the laser was passed through a 2-mm-thick Schott WG-290 filter to remove the 275-nm line also produced by this laser in the deep-UV mode. In both cases, emission was collected through a Schott WG-345 cut-on filter and a Corning 7-54 band-pass filter. All titration experiments were performed in 50 mM EPPS-KOH (pH = 8.0), 10 mM $MgCl_2$, 10 mM NH_4Cl, and 0.2 mM EDTA, with a blank correction for the buffer made in both intensity and anisotropy studies. PFK subunit concentration was equal to 4.2−5.7 μM (0.15−0.2 mg/mL) for all steady-state measurements.

Frequency-Domain Fluorescence Measurements. Frequency domain fluorometry was performed on the ISS K2, using the 300-nm line of the Spectra-Physics argon ion laser described above. Emission and excitation filters and buffer conditions were identical to those described for the steady-state fluorescence measurements, while the PFK subunit concentration was 5.7−8.6 μM. All measurements were performed in a 1 × 1 cm cuvette with continuous stirring to minimize sample photobleaching. Blank correction was not performed because the signal contributed by the buffer was less than 3% in all cases. Data analysis was performed with Globals Unlimited, obtained from the Laboratory for Fluorescence Dynamics at the University of Illinois at Urbana−Champaign.

Iodide Quenching. Frequency-domain phase and modulation measurements were performed on each of the six enzyme forms individually in the presence of 0, 0.05, 0.1, and 0.15 M KI. Controls have shown that increases in ionic strength accompanying the addition of concentrations of KCl as high as 0.25 M failed to alter the fluorescence lifetime of the PFK ligated with the various combinations of PEP and Fru-6-P (data not shown). All data sets were globally linked in terms of the percent of each species in solution and fit using the Globals Unlimited program to the following equation:

$$\frac{\tau^0}{\tau} = 1 + \tau^0 k_q[I^-] \qquad (1)$$

where τ^0 represents the lifetime in the absence of quencher, τ represents the apparent lifetime at a given concentration of iodide, and k_q is the bimolecular collisional rate constant pertaining to the collision of I^- with the excited state of the fluorescent species. The Stern−Volmer constant, K_{sv}, obtained directly from the slope of τ^0/τ vs $[I^-]$, represents the product of τ^0 and the bimolecular rate constant k_q.

Measurements of Ligand Binding. In the absence of either MgATP or Fru-6-P, i.e., when there is no catalytic activity from PFK, either the intensity and/or the polarization of the intrinsic fluorescence derived from the single tryptophan moiety present in each subunit has been found to provide a good monitor of ligand binding. Variation in these param-

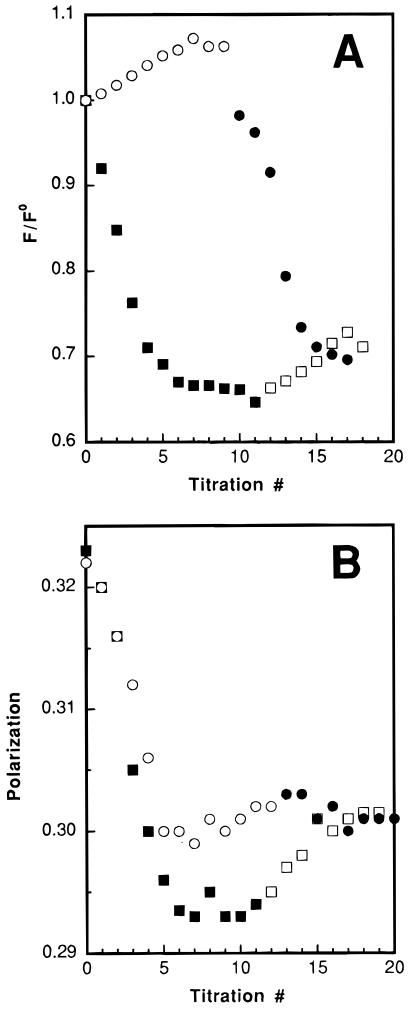

FIGURE 1: (A) Changes in the steady-state intensity of *E. coli* PFK's intrinsic fluorescence induced by Fru-6-P and PEP in the absence of MgATP. When binding to free PFK, Fru-6-P (■) causes a 36% decrease and PEP (○) causes a 9% increase in fluorescence intensity. PEP titrated into PFK previously saturated with Fru-6-P (□) increases intensity by 6%, while Fru-6-P induces a 40% decrease in the intensity of PFK previously saturated by PEP (●). Regardless of the order of addition, a ternary complex is generated approximately 30% lower in intensity than free PFK. (B) Changes induced by Fru-6-P and PEP in the steady-state polarization of the intrinsic tryptophan of *E. coli* PFK in the absence of MgATP. Absolute changes in polarization of 0.03 and 0.02 accompany the saturation of PFK by Fru-6-P (■) and PEP (○), respectively. Additions of Fru-6-P to PFK previously saturated with PEP (●) generate a polarization describing the ternary complex identical to that produced by additions of PEP to PFK previously saturated with Fru-6-P (□).

eters induced by MgATP and Fru-6-P has earlier been presented (Johnson & Reinhart, 1992, 1994a). As seen in Figure 1A, the intrinsic fluorescence intensity is quite responsive to binding by Fru-6-P and PEP. Fru-6-P causes a 36% drop, while PEP binding promotes a small increase (9%). When Fru-6-P binds after PEP, a large decrease in intensity of approximately 40% results. In the reverse situation, when PEP is introduced after Fru-6-P has bound, fluorescence intensity increases slightly (6%) to a value representative of the ternary complex. All intensity data were adjusted for the inner filter effect brought about by titration of large concentrations of PEP required for saturation (Lakowicz, 1983).

The pattern of ligand-induced changes is quite different when the fluorescence polarization of the intrinsic tryptophan is monitored, as indicated in Figure 1B. Instead of inducing opposite changes in the fluorescence parameter, the binding of both Fru-6-P and PEP decreases the intrinsic polarization, although to different extents. Fru-6-P induces a change of approximately 0.03, while PEP lowers the polarization value by about 0.02. The ternary complex of allosteric inhibitor and substrate exhibits a steady-state polarization essentially identical to that of the PEP-bound complex.

Quantifying the Allosteric Actions of PEP. There are three relevant ligands to consider in a complete linked-function description of PEP's influence on PFK activity: Fru-6-P, MgATP, and PEP. We designate these ligands as A, B, and Y, respectively.

In order to quantify the overall effect of PEP on the binding of another ligand, it is necessary to determine the coupling parameter between the two ligands; for example, the coupling between Fru-6-P and PEP, designated Q_{ay}, is defined as follows:

$$Q_{ay} = \frac{K^0_{ia}}{K_{ia/y}} = \frac{K^0_{iy}}{K_{iy/a}} \tag{2}$$

where K^0_{ia} represents the dissociation constant of substrate (A) in the absence of any allosteric ligand, $K_{ia/y}$ represents the dissociation constant of substrate when PEP (Y) is fully saturating, K^0_{iy} represents the dissociation constant of PEP in the absence of any other ligand, and $K_{iy/a}$ represents the dissociation constant of PEP when substrate is saturating. Other coupling constants, for example, between MgATP and PEP, Q_{by}, and between Fru-6-P and MgATP, Q_{ab}, are defined analogously. In this notation the ligand designation following the slash mark identifies the ligands that are saturating. Consequently, to ascribe a coupling between two ligands while another ligand is saturating under all conditions, a slash mark followed by the letter designation for the saturating ligand is used. For example, the coupling between Fru-6-P and PEP when MgATP is saturating is represented by $Q_{ay/b}$, defined as follows:

$$Q_{ay/b} = \frac{K_{ia/b}}{K_{ia/by}} = \frac{K_{iy/b}}{K_{iy/ab}} \tag{3}$$

These coupling parameters were determined by measuring the dependence of the apparent dissociation constant for one ligand on the concentration of the second ligand and fitting these data to eq 4 as described previously (Reinhart, 1983, 1985; Reinhart & Hartleip, 1987, 1992; Braxton et al., 1992; Symcox & Reinhart, 1992).

$$K_{0.5} = K^0_{ia}\left(\frac{K^0_{iy} + [Y]}{K^0_{iy} + Q_{ay}[Y]}\right) \tag{4}$$

The notation in eq 4 specifically pertains to Fru-6-P and PEP as indicated above. The apparent dissociation constant for Fru-6-P is designated $K_{0.5}$, reflecting the potential for cooperativity in the Fru-6-P binding profiles.

In a mechanism in which substrate and allosteric inhibitor bind mutually exclusively to R and T states, respectively, the value of $K_{0.5}$ increases without limit as [Y] increases, and Q_{ay} is therefore equal to 0. In this case, eq 4 reduces to the following form:

$$K_{0.5} = K_{ia}^{0}\left(\frac{K_{iy}^{0} + [Y]}{K_{iy}^{0}}\right) = K_{ia}^{0}\left(1 + \frac{[Y]}{K_{iy}^{0}}\right) \quad (5)$$

All other procedural details pertaining to equation fitting and data analysis have been described previously (Johnson & Reinhart, 1994a).

Generation of Enzyme Ligand Forms. Enzyme complexes analyzed in steady-state and dynamic fluorescence studies were generated by the following additions: 0.5 mM Fru-6-P to generate PFK−F6P; 10 mM PEP to generate PEP−PFK; and both 20 mM Fru-6-P and 60 mM PEP to generate PEP−PFK−F6P. For the binary complexes, these ligand concentrations are greater than 100 times the relevant K_d. For the PEP−PFK−F6P ternary complex, these concentrations of Fru-6-P and PEP were shown to be sufficient to fully achieve a plateau value in intrinsic fluorescence intensity when either ligand was varied around these concentrations.

RESULTS

Characterization of Coupling Parameters

Fru-6-P−PEP Coupling in the Saturating Presence of MgATP. It has been previously established that PEP acts as a K-type effector in its inhibition of *E. coli* PFK; i.e., it antagonizes Fru-6-P binding without influencing k_{cat} (Blangy et al., 1968). We have confirmed that, even under saturating concentrations of PEP, k_{cat} is virtually constant (data not shown). To quantify the magnitude of the allosteric effect PEP exerts on Fru-6-P binding when MgATP is saturating, values of $K_{0.5}$ for Fru-6-P were determined at PEP concentrations ranging from 0 to 60 mM by monitoring PFK activity with [MgATP] = 3 mM. The data obtained are depicted in Figure 2. These data were fit via nonlinear regression analysis to eq 4 to provide the value of the coupling between Fru-6-P and PEP when MgATP is saturating, $Q_{ay/b}$. The solid line in Figure 2 corresponds to this fit, while the dashed line represents the best fit to eq 5, which represents a model in which Fru-6-P and PEP cannot bind to the same enzyme form. It is clear that eq 4 does a much better job of describing the data.

$K_{0.5}$ determined in this manner will yield thermodynamic parameters if the value of the off-rate constant for the substrate from both the substrate−enzyme complex and the ternary complex of substrate, effector, and enzyme is very large relative to the value of k_{cat}. The veracity of this rapid-equilibrium condition for Fru-6-P was evaluated using a simple steady-state kinetic method performed under solution conditions identical to those of normal kinetic assays (Symcox & Reinhart, 1992). In this method, independent experimental determinations of $Q_{ay/b}$ are made by both measurements of $K_{0.5}$ as a function of PEP concentrations and of the apparent dissociation constant for PEP (K_y) as a function of Fru-6-P concentration. If these values of $Q_{ay/b}$ are equal, then the rapid equilibrium assumption is valid (Symcox & Reinhart, 1992). The variation of K_y with Fru-6-P determined in this manner is presented in Figure 3. The two plateau values evident in Figure 3 allow estimates to be made for $K_{iy/b}$ and $K_{iy/ab}$, from which a value of $Q_{ay/b}$ was calculated according to eq 2. This value of $Q_{ay/b}$ agrees well with the value determined from the data presented in Figure 2 as indicated by the double-headed arrow in Figure 3.

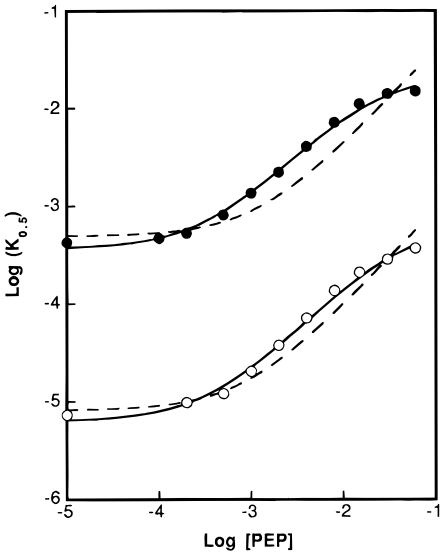

FIGURE 2: Variation of log K_a for Fru-6-P with the log of PEP concentration at 0 (○) and 3 mM (●) MgATP. K_a values are represented either by $K_{0.5}$ determined kinetically in the presence of MgATP or by K_d determined via fluorescence intensity in the absence of MgATP (Figure 1A). Solid lines represent the best fit of these data to eq 4. Dashed lines represent the best fit of these data to eq 5. Values of Q_{ay} and $Q_{ay/b}$ deriving from the fit of eq 4 are summarized in Table 2.

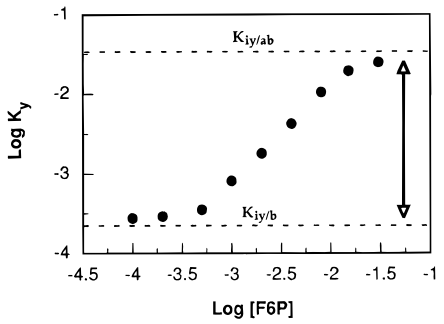

FIGURE 3: Variation of log K_y for PEP with the log of Fru-6-P concentration. K_y values were determined by following the inhibition of enzymatic activity by PEP at various Fru-6-P concentrations when MgATP concentrations were fixed at 3 mM. The cooperativity of Fru-6-P binding prevented these data from being fit to eq 4, but estimates were made for the limiting values of K_y (dashed lines). The magnitude of $Q_{ay/b}$ determined from limiting values of K_a (Figure 2) is represented by the vertical arrow, and its similarity to the magnitude of $Q_{ay/b}$ based upon approximations for the limiting values of K_y suggests that Fru-6-P binds in rapid equilibrium during the enzymatic turnover of *E. coli* PFK.

Therefore we conclude that the rapid-equilibrium condition is met, consistent with our earlier prediction (Johnson & Reinhart, 1992).

Fru-6-P−PEP Coupling in the Absence of MgATP. Using the quenching of PFK's intrinsic tryptophan fluorescence as a probe (Figure 1A), we determined K_{ia} for Fru-6-P in the absence of MgATP at concentrations of PEP ranging from 0 to 60 mM. These data are also summarized in Figure 2, with the solid line corresponding to the best fit of these data to eq 4 to yield the value for Q_{ay}. The couplings are evident by inspection from the differences between the two plateaus for each curve. The results clearly indicate that, despite the substantial antagonism between Fru-6-P and MgATP (evident by the vertical displacement of the two curves), MgATP has very little effect on the ability of PEP to further antagonize the binding of Fru-6-P. The dashed line represents the best

Table 1: Ligand Dissociation Constants from *E. coli* PFK for All Combinations of Fru-6-P, MgATP, and PEP at 25 °C

ligand	other saturating ligands	designation	K_d (μM)
Fru-6-P		K_{ia}^0	4.5 ± 0.3[a]
Fru-6-P	MgATP	$K_{ia/b}$	420 ± 20[a]
Fru-6-P	PEP	$K_{ia/y}$	410 ± 80
Fru-6-P	MgATP, PEP	$K_{ia/by}$	$(2.6 \pm 0.6) \times 10^4$
MgATP		K_{ib}^0	0.025 ± 0.004[a]
MgATP	Fru-6-P	$K_{ib/a}$	1.7 ± 0.3[a,b]
MgATP	PEP	$K_{ib/y}$	0.019 ± 0.003
MgATP	Fru-6-P, PEP	$K_{ib/ay}$	0.89 ± 0.10
PEP		K_{iy}^0	240 ± 20
PEP	Fru-6-P	$K_{iy/a}$	$(2.2 \pm 0.6) \times 10^4$
PEP	MgATP	$K_{iy/b}$	185 ± 22
PEP	Fru-6-P, MgATP	$K_{iy/ab}$	$(1.2 \pm 0.4) \times 10^4$

[a] As reported by Johnson and Reinhart (1992, 1994a). [b] MgATP does not achieve rapid equilibrium during catalytic turnover ($K_m = 49$ μM).

Table 2: Fru-6-P/MgATP/PEP Coupling Constants (Q) That Quantify the Interactions between Fru-6-P, MgATP, and PEP on *E. coli* PFK at 25 °C

interacting ligands	other saturating ligand	designation	Q
Fru-6-P−PEP		Q_{ay}	0.011 ± 0.003
Fru-6-P−PEP	MgATP	$Q_{ay/b}$	0.016 ± 0.002[a]
MgATP−PEP		Q_{by}	1.3 ± 0.1
MgATP−PEP	Fru-6-P	$Q_{by/a}$	1.9 ± 0.6
Fru-6-P−MgATP		Q_{ab}	0.015 ± 0.001[b]
Fru-6-P−MgATP	PEP	$Q_{ab/y}$	0.022 ± 0.007
Fru-6-P−MgATP−PEP		Q_{aby}	0.00031 ± 0.00005

[a] A value of 0.012 was determined for $Q_{ay/b}$ via a variation in K_y vs [Fru-6-P]. [b] As reported by Johnson and Reinhart (1992, 1994a).

agreement of these data to eq 5, describing the mutually exclusive two-state model. Clearly this function does a poor job of describing the data as well.

MgATP−PEP Coupling in the Saturating Presence of Fru-6-P. Measurements of the potential influence of PEP on the thermodynamic binding of MgATP in the presence of Fru-6-P is not possible, since MgATP does not achieve binding equilibrium in the steady state (Johnson & Reinhart, 1992). The magnitude of this allosteric interaction may be deduced from other couplings, however, as described below. To ensure that PEP does not compete at the MgATP active site in a manner analogous to MgADP, the impact on V_{max} and the K_m for MgATP by PEP was investigated, with Fru-6-P maintained at saturating concentrations. Neither K_m for MgATP nor V_{max} is significantly influenced by the presence of PEP in solution (data not shown).

MgATP−PEP Coupling in the Absence of Fru-6-P. By titrating PEP and following the concomitant decrease in the fluorescence polarization of Trp311 in *E. coli* PFK, apparent values of K_{iy}^0 for PEP were determined at various concentrations of MgATP ranging from 5 to 500 μM (data not shown). Because of the very high affinity of MgATP for free PFK (25 nM; Johnson & Reinhart, 1992), MgATP proved to be saturating at all concentrations examined. The ratio of dissociation constants for PEP in the absence and saturating presence of MgATP provide the value of Q_{by} (eq 2). MgATP increased the binding affinity for PEP by only 30%. Linkage reciprocity requires that PEP have an equally small effect on MgATP binding.

All of the dissociation constants and coupling constants measured as described above are listed in Tables 1 and 2. The remaining coupling constants can be calculated as follows.

The magnitude of the coupling between Fru-6-P and MgATP, Q_{ab}, has been previously determined to be equal to 0.015 ± 0.001 (Johnson & Reinhart, 1992). With this value and the values of Q_{ay}, $Q_{ay/b}$, and Q_{by} determined from the results presented in this report, a complete linked-function analysis of all other potential couplings between Fru-6-P, PEP, and MgATP, may be calculated. The principles of thermodynamic linkage give rise to the following identities (Reinhart, 1983, 1988):

$$Q_{aby} \equiv \frac{K_{ia}^0 K_{ib}^0 K_{iy}^0}{K_{ia}^0 K_{ib/a} K_{iy/ab}} = Q_{ab} Q_{by} Q_{ay/b} \quad (6)$$

$$Q_{by/a} = \frac{Q_{aby}}{Q_{ay} Q_{ab}} \quad (7)$$

$$Q_{ab/y} = \frac{Q_{aby}}{Q_{ay} Q_{by}} \quad (8)$$

As indicated in eq 6, Q_{aby} is the coupling associated with the binding of three ligands to separate sites (Reinhart, 1988). Values for Q_{aby}, $Q_{by/a}$ (the coupling between MgATP and PEP at saturating Fru-6-P), and $Q_{ab/y}$ (the coupling between Fru-6-P and MgATP at saturating PEP) determined by the use of these equations are presented in Table 2.

van't Hoff Analyses of Allosteric Responses. The coupling constants describing the allosteric action by PEP are equilibrium constants for the following disproportionation reactions (Weber, 1972, 1975):

$$\text{PFK–F6P + PEP–PFK} \overset{Q_{ay}}{\rightleftharpoons} \text{PFK + PEP–PFK–F6P} \quad (9)$$

$$\begin{array}{ccc} \text{PFK + PEP–PFK} & \overset{Q_{by}}{\rightleftharpoons} & \text{PFK + PEP–PFK} \\ | & & | \\ \text{MgATP} & & \text{MgATP} \end{array} \quad (10)$$

$$\begin{array}{ccccc} \text{PFK–F6P + PEP–PFK} & \overset{Q_{ay/b}}{\rightleftharpoons} & \text{PFK + PEP–PFK–F6P} \\ | \quad\quad | & & | \quad\quad | \\ \text{MgATP} \quad \text{MgATP} & & \text{MgATP} \quad \text{MgATP} \end{array} \quad (11)$$

Q_{ay}, Q_{by}, and $Q_{ay/b}$ can each be converted into the corresponding coupling free energy by eq 12, specifically given for the coupling between Fru-6-P and PEP in the absence of MgATP:

$$\Delta G_{ay} = -RT \ln (Q_{ay}) = \Delta H_{ay} - T\Delta S_{ay} \quad (12)$$

where R is the gas constant and T is the temperature in kelvins. In the absence of a significant change in heat capacity, the constituent van't Hoff enthalpy (ΔH_{ay}) and entropy (ΔS_{ay}) contributions that give rise to the coupling parameters can be ascertained from the temperature dependence of Q_{ay} (Reinhart et al., 1989; Braxton et al., 1994; Johnson & Reinhart, 1994a).

At temperatures ranging from 5 to 35 °C, values for the coupling between Fru-6-P and PEP in the absence and presence of bound MgATP, Q_{ay} and $Q_{ay/b}$, respectively, were determined as described above. Figure 4 presents a plot of log Q versus reciprocal temperature expressed in kelvins. In both cases, plots are linear and the values of the coupling

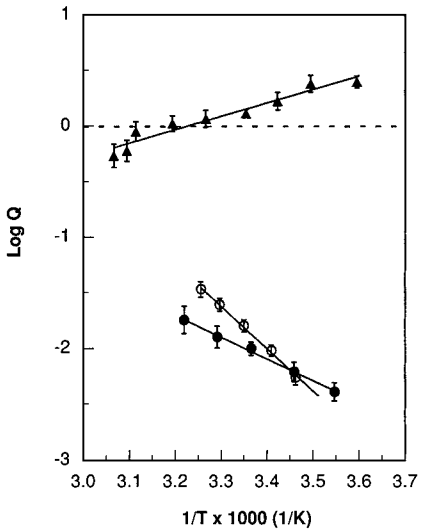

FIGURE 4: van't Hoff analysis of the coupling between Fru-6-P and PEP in the absence (●, Q_{ay}) and saturating presence (○, $Q_{ay/b}$) of MgATP and of the coupling between MgATP and PEP in the absence of Fru-6-P (▲, Q_{by}). The log of Q_{ay}, $Q_{ay/b}$, and Q_{by} vary linearly vs reciprocal temperature to provide values for coupling enthalpy and entropy for each (Reinhart & Johnson, 1994a). Although both Q_{ay} and $Q_{ay/b}$ are similar at 25 °C, increases in temperature reveal differences in the thermodynamic properties of the two couplings. PEP enhances MgATP binding at low temperatures, but it becomes an inhibitor of MgATP binding at temperatures greater than approximately 40 °C as indicated by the negative values of log Q_{by}.

Table 3: Thermodynamic Parameters Governing Allosteric Couplings in *E. coli* PFK

coupling	ΔG at 25 °C (kcal/mol)	ΔH (kcal/mol)	$T\Delta S$ at 25 °C (kcal/mol)
Q_{ay}	$+2.7 \pm 0.1$	$+9.1 \pm 1.3$	$+6.4 \pm 1.3$
$Q_{ay/b}$	$+2.4 \pm 0.2$	$+17.2 \pm 1.8$	$+14.8 \pm 1.8$
Q_{by}	-0.2 ± 0.03	-5.2 ± 0.6	-5.0 ± 0.6
$Q_{by/a}$	-0.5 ± 0.1	$+2.9 \pm 0.8$	$+3.4 \pm 0.8$
Q_{ab}	$+2.5 \pm 0.2$[a]	$+8.5 \pm 1.3$[a]	$+6.0 \pm 1.3$[a]
$Q_{ab/y}$	$+2.2 \pm 0.5$	$+16.6 \pm 0.9$	$+14.4 \pm 0.9$
Q_{aby}	$+4.7 \pm 0.9$	$+20.5 \pm 1.1$	$+15.8 \pm 1.1$

[a] As reported by Johnson and Reinhart (1994a).

constants are augmented by increased temperatures (i.e., inhibition decreases as temperature increases). The best weighted linear-regression fit to these data provide the values presented in Table 3.

The coupling between MgATP and PEP (Q_{by}) was examined similarly, at temperatures ranging from 5 to 53 °C, and these data are also presented in Figure 4. In this case the slight activation of binding affinity engendered by one ligand on the other at 25 °C is magnified about 2-fold when the temperature is lowered to 5 °C. Elevated temperatures, however, *reverse the allosteric response* of PFK to these ligands, with MgATP *antagonizing* PEP affinity by about 2-fold at 53 °C.

Fluorescence Characterization of Enzyme Conformations

Determination of Fluorescence Decay Times. There are four individual complexes appearing in the disproportionation equilibrium for Q_{ay} (eq 9) whose relative characteristics define the relationship between Fru-6-P and PEP in the absence of MgATP: free PFK, binary complexes of PFK bound to either Fru-6-P or PEP, and the ternary complex of PFK to which both Fru-6-P and PEP are bound. Using frequency-domain fluorometry, we investigated the lifetime of fluorescence decay of the intrinsic tryptophan in each complex (data not shown). Each data set is best described by a model of two discrete exponential decays, with greater than 92% of the fluorescence deriving from the longer lifetime under all circumstances. Consistent with data reported previously describing the actions of MgADP (Johnson & Reinhart, 1994b), the decay time of the smaller percentage component is independent of binding by Fru-6-P and/or PEP. Consequently, this decay time was linked across all four data sets during global analysis ($\chi^2 = 3.6$) and a value of 2.10 ± 0.12 ns for this short component was obtained. However, the remaining lifetime describing PFK's intrinsic tryptophan emission varies with the state of ligation for each of the four enzyme complexes, as summarized in Table 4. These values qualitatively agree with changes in steady-state intensity observed upon PFK binding to Fru-6-P and PEP, individually and in combination (Figure 1A).

Iodide Quenching Studies. The influence of iodide ions on the long-component fluorescence lifetime was measured for each of the four species in the disproportionation equilibrium describing Q_{ay}. As predicted by the collisional quenching model that gives rise to eq 1, τ^0/τ varies linearly with [KI] (data not shown). For each enzyme form all of the frequency-domain data collected at each iodide concentration were fit to eq 1 using the Globals Unlimited program and the resulting values of k_q, the bimolecular collisional quenching rate constant, are given in Table 4. All ligated species of PFK were more exposed to quenching than free PFK, with PFK−F6P exhibiting the largest value for k_q , PEP−PFK exhibiting a small increase, and the value for the ternary complex intermediate between those for PFK−F6P and PEP−PFK.

Steady-State Fluorescence Polarization. The isothermal variation of solution viscosity leads to changes in the global rotational rate of a macromolecule in solution, which can be detected by measurements of steady-state polarization (Weber, 1952a,b). Additions of viscogens, however, typically do not alter the faster local rotations of limited amplitude often associated with the reporter residue or dye attached to a protein. Plots of reciprocal polarization versus T/η, where η represents viscosity, may be extrapolated to infinite viscosity to provide values for the apparent limiting polarization, P_0 (Weber, 1952a), and the value of this parameter will be influenced by the degree of local motion experienced by the reporter group. This type of analysis, termed a Perrin plot, was performed on each of the four enzyme complexes relevant to net inhibition of Fru-6-P binding by PEP (data not shown). Each data set fit well to a straight line, and changes in the tryptophan rotation between each enzyme form were detected by the changes in the intercepts of the Perrin plots. The resulting values for P_0 are presented in Table 4. Moreover, the Perrin plots were parallel, indicating that the binding of the various combinations of Fru-6-P and PEP does not significantly alter the rotational relaxation times of *E. coli* PFK as a whole, but instead predominantly changes either the amplitudes or rates of rotation for the tryptophan side chain. Energy transfer, which can also lead to changes in the apparent P_0, is not likely to be the cause of these results because the potential for Trp → Trp transfer has been minimized by exciting at the red edge (300 nm) of tryptophan absorption.

Table 4: Biophysical Parameters Describing Enzyme Complexes Relevant to the Inhibition by PEP of Fru-6-P Binding to *E. coli* PFK[a]

complex	τ[b] (ns)	f_1	P_0	k_q (M·ns)$^{-1}$	$r_0 - r_\infty$[c]	Φ (deg)
PFK	6.13 ± 0.09	0.94 ± 0.01	0.362 ± 0.002	0.13 ± 0.03	0.045 ± 0.014	21 ± 4
PFK−Fru-6-P	5.31 ± 0.08	0.92 ± 0.01	0.325 ± 0.002	0.33 ± 0.04	0.142 ± 0.013	42 ± 2
PEP−PFK	6.32 ± 0.10	0.94 ± 0.01	0.336 ± 0.001	0.16 ± 0.03	0.053 ± 0.013	23 ± 3
Fru-6-P−PFK−PEP	5.55 ± 0.09	0.93 ± 0.01	0.333 ± 0.001	0.27 ± 0.03	0.079 ± 0.012	29 ± 2

[a] Symbols used in this table correspond to the following parameters: τ, fluorescence lifetime of major component; f_1, fractional intensity of the major component; P_0, apparent limiting polarization as measured by Perrin plots; k_q, bimolecular rate constant pertaining to quenching by I^-; $r_0 - r_\infty$, preexponential amplitude for fast rotation; and Φ, cone angle of local rotation for the indole moiety. [b] Data were analyzed with a second lifetime component, τ_2, linked across all data sets. $\tau_2 = 2.10 \pm 0.12$ ns; global $\chi^2 = 3.60$. [c] The parameters ϕ_1, ϕ_2, and r_0 were linked across all data sets and found to be equal to 0.83 ± 0.32 ns, 72 ± 9 ns, and 0.26 ± 0.03, respectively. Global $\chi^2 = 0.95$.

Frequency-Domain Anisotropy. The differential phase and modulation associated with each of the four enzyme complexes relevant to Q_{ay} (i.e., eq 9), when presented as a function of the frequency of the intensity modulation of the excitation source, illustrate the differences between fast and slow rotations for the tryptophan, evident at high and low frequencies, respectively. Additionally, with these data one potentially can discriminate between contributions to the extent of depolarization by either the amplitude ($r_0 - r_\infty$) or the rate (ϕ_1) of the fast local rotation. The data fit well to a model described by eq 13, which allows for a hindered local plus unhindered global protein rotation (Munro et al., 1979; Lipari & Szabo, 1980; Johnson & Reinhart, 1994b):

$$r(t) = (r_0 - r_\infty)\, e^{-t/\phi_1} + r_\infty\, e^{-t/\phi_2} \qquad (13)$$

The results indicated that there is little to no variation in either global (ϕ_2) or local (ϕ_1) rotational relaxation times detected between the four enzyme complexes. For this reason a global analysis was performed of all data sets in which these parameters, as well as the limiting anisotropy r_0, were linked across the data sets. Lifetimes were fixed to those established as described above. The primary distinction between the rotational characteristics of the tryptophan in each of the enzyme species was found to lie in differences between the amplitude of local rotation, as summarized in Table 4. The other parameters were linked in the analysis and were determined to have the following values ($\chi^2 = 0.95$): $\phi_2 = 72 \pm 9$ ns; $\phi_1 = 0.83 \pm 0.32$ ns; and $r_0 = 0.26 \pm 0.03$.

The amplitude of local motion, in turn, may be described in terms of a cone angle of limited rotation (Φ) available to the tryptophan side chain in each enzyme complex by eq 14 (Munro et al., 1979; Lipari & Szabo, 1980; Gratton et al., 1986; Johnson & Reinhart, 1994). The parameters appearing in eq 14—r_0, the limiting anisotropy observed in the absence of all depolarizing processes, and r_∞, the limiting anisotropy observed at times that are long compared to the fluorescence lifetime—are provided by analysis of the frequency reponse.

$$\cos(\Phi) = \left[\left(1 + 3\left(\frac{r_\infty}{r_0}\right)^{1/2}\right)^{1/2} - 1\right] \qquad (14)$$

Calculated cone angles are summarized in Table 4.

DISCUSSION

The appropriateness of a two-state model must be considered from both functional and structural perspectives. The data presented in Figure 2 clearly indicate that an exclusive, two-state model is insufficient to describe the inhibitory effects of PEP and MgATP on PFK from *E. coli*. In both the absence and presence of MgATP, plateau values of $K_{0.5}$ for Fru-6-P are clearly approached at high concentrations of PEP, indicating the formation of a PEP−PFK−F6P ternary complex at high concentrations of both ligands. This enzyme form does not functionally correspond to either R or T since it exhibits a low affinity for both PEP and Fru-6-P while having an unaltered k_{cat}.

It is also clear from the data presented in Figure 2 that MgATP has little influence on the inhibition by PEP of Fru-6-P binding at 25 °C. The coupling constant between Fru-6-P and PEP in the absence of MgATP ($Q_{ay} = 0.011$) is comparable in magnitude to that of the same coupling in the presence of MgATP ($Q_{ay/b} = 0.016$). Similarly, PEP has little influence on the inhibition of Fru-6-P binding by MgATP ($Q_{ab} = 0.015$, $Q_{ab/y} = 0.022$). Moreover, in light of the fact that MgATP and PEP are not antagonistic relative to one another but rather have very little influence on each other's binding ($Q_{by} = 1.3$), it is clear that *PEP and MgATP inhibit the binding of Fru-6-P by completely different, virtually independent mechanisms*. This result is also inconsistent with the two-state model.

Although the magnitude of Fru-6-P inhibition by PEP is essentially unaltered by the presence of MgATP at 25 °C, analysis of the temperature dependence of Q_{ay} and $Q_{ay/b}$ demonstrates a significant impact by MgATP on the thermodynamics of these interactions as shown in Figure 4 and Table 3. In the saturating presence of MgATP, both the coupling enthalpy ($\Delta H_{ay/b}$) and entropy ($\Delta S_{ay/b}$) are substantially increased relative to those measured in its absence. In both cases, there is a positive sign for coupling enthalpy, which favors inhibition, and a positive sign for coupling entropy, which favors PEP activation (eq 12). It is only because the two thermodynamic forces oppose one another that a coupling free energy results from $Q_{ay/b}$ at 25 °C similar to that from Q_{ay}. As temperature is elevated, however, PEP becomes a much less potent inhibitor of Fru-6-P in the presence of MgATP than in its absence, attributable to the greater weight being given by temperature to the larger $T\Delta S_{ay/b}$ term favoring PEP activation.

The delicate interplay between large absolute values of coupling entropy and enthalpy that give rise to relatively small values of coupling free energy is perhaps most dramatically demonstrated with regard to the influence of temperature on Q_{by}. The slight activation between MgATP and PEP at 25 °C ($Q_{by} > 1$) is switched to inhibition in response to higher temperatures; i.e., the very nature of the allosteric response is reversed. Such temperature-induced inversion of an allosteric effect has earlier been reported for the allosteric effectors MgADP in *B. stearothermophilus* PFK and IMP in *E. coli* carbamoyl phosphate synthetase, both of which turned from K-type activators to inhibitors with

decreasing temperatures (Braxton et al., 1994). Functionally, such behavior is most straightforwardly rationalized as a simple property of the corresponding disproportionation equilibrium (eq 10) and the chemical potentials of *all* of the species participating in that reaction.

From a structural point of view, the issue is whether the functionally defined "free enzyme" and "ternary complex" represent simply mixtures of structures that are essentially defined by the structural properties of the Fru-6-P-bound and PEP-bound forms. Although an X-ray crystallographic structure of the latter has not yet been determined for PFK from *E. coli*, a structure with a PEP analogue (phosphoglycolate) bound has been determined for the homologous enzyme from *B. stearothermophilus* (Schirmer & Evans, 1990). This structure exhibits significant structural alterations compared to structures with Fru-6-P and MgADP bound, which has led to the proposal that these structural differences can explain the inhibition behavior.

A structure for free PFK from *E. coli* has been determined (Rypniewski & Evans, 1989) and been found to be structurally similar to that of the Fru-6-P-bound or R form (Shirakihara & Evans, 1988) despite previous expectations that free enzyme adopts the T form since Fru-6-P binding exhibits positive cooperativity. Deville-Bonne and Garel (1992) have suggested, in order to describe the opposing effects on steady-state fluorescence intensity by Fru-6-P and PEP relative to free enzyme within the context of a two-state model, that PFK without ligands present exists as a mixture of $^1/_3$ R and $^2/_3$ T. Although the steady-state intensity changes (and associated lifetime changes) of PFK's intrinsic tryptophan concomitant to the binding of Fru-6-P and PEP are opposite in nature (Figure 1A, Table 4), the steady-state polarizations of both PFK−F6P and PEP−PFK are both much lower than those of free enzyme (Figure 1B). Similarly, PFK bound individually to either Fru-6-P or PEP exhibits higher values for the bimolecular rate constant, k_q, associated with I^- quenching than free PFK, indicating that the tryptophan side chain of free enzyme is less accessible to I^- in bulk solution than it is when ligands are bound. Also, the characteristics of the local motion associated with the tryptophan side chain in the free enzyme, as revealed by P_0, $(r_0 - r_\infty)$, and Φ, all fall outside a range defined by PEP−PFK and PFK−F6P (Table 4). Certainly, these data challenge the notion that free enzyme exists as some equilibrium mixture of two forms comparable to the two forms that result from the binding of Fru-6-P and PEP, respectively.

The structural nature of PEP−PFK−F6P is unfortunately more ambiguous. It is possible that the ternary complex actually represents an equilibrium mixture of two species in equilibrium since each of the parameters associated with the ternary complex listed in Table 4 has a value that is intermediate between limits set by PEP−PFK and PFK−F6P. However, such a presumption is at best arbitrary since the data do not require this complication to be explained. According to Occam's razor, it is simpler to consider the ternary complex to exhibit structural features that are intermediate between limits set by PEP−PFK and PFK−F6P relative to those attributes addressed by the data in Table 4.

Of course it is difficult to know *a priori* whether these differences in protein flexibility, detected in the vicinity of the tryptophan side chain, are relevant to the function of the enzyme, especially considering that the tryptophan is located approximately 20 Å from either the active site or the allosteric site. However, if these perturbations reflect systemic changes in protein flexibility, they could impact coupling entropy. As indicated by the temperature dependence of the MgATP−PEP coupling shown in Figure 4, coupling entropy can influence the nature as well as the magnitude of an allosteric response. Coupling entropy can include differences in the degree of conformational degeneracy between the sum of enzyme forms on opposite sides of the disproportionation equilibria describing net allosteric effects such as those given in eqs 9−11 (Cooper & Dryden, 1984; Reinhart et al., 1989; Johnson & Reinhart, 1994b; Braxton et al., 1996). A positive sign for ΔS_{ay}, for example, may indicate that the flexibility and associated ability to populate various configurational substates of PEP−PFK−F6P + PFK is greater than that of PFK−F6P + PEP−PFK (eq 9).

This hypothesis has previously been explored by calculating the cone angles of local tryptophan rotation (Φ) in each of the enzyme complexes appearing in the disproportionation equilibria for MgADP activation of Fru-6-P binding and inhibition of MgATP binding and comparing the combined flexibility as described by Φ of the respective enzyme forms to the signs of ΔS_{ax} and ΔS_{bx} (Johnson & Reinhart, 1994b).[2] In those previous cases, a correlation was found to exist between the signs of the coupling ΔS and the modest changes in the amplitude of the cone angle that represents the amplitude of the flexibility of the tryptophan side chain. From the data presented here, a comparable simple correlation does not appear to exist with the enzyme forms involved in the coupling between Fru-6-P and PEP. However, a single tryptophan may not necessarily be representative of global protein characteristics in all cases, and a more comprehensive study of the influence of ligand binding on PFK's internal dynamics is presently underway. It should be emphasized, however, that given the frequency with which coupling entropy has been found to have a major influence on the nature and magnitude of allosteric action, changes in protein conformational flexibility must be considered when interpreting the functional impact of ligand binding and any ensuing conformational change.

[2] Inadvertently, cone half-angles were reported in Johnson and Reinhart (1994b). To compare to the values listed in Table 4, the values reported in Johnson and Reinhart (1994b) should be multiplied by 2.

REFERENCES

Berger, S. A., & Evans, P. R. (1991) *Biochemistry 30*, 8477−8480.
Blangy, D., Buc, H., & Monod, J. (1968) *J. Mol. Biol. 31*, 13−35.
Braxton, B. L., Mullins, L. S., Raushel, F. M., & Reinhart, G. D. (1992) *Biochemistry 31*, 2309−2316.
Braxton, B. L., Tlapak-Simmons, V. L., & Reinhart, G. D. (1994) *J. Biol. Chem. 269*, 47−50.
Braxton, B. L., Mullins, L. S., Raushel, F. M., & Reinhart, G. D. (1996) *Biochemistry 35*, 11918−11924.
Cooper, A., & Dryden, D. T. F. (1984) *Eur. Biophys. J. 11*, 103−109.
Deville-Bonne, D., & Garel, J.-R. (1992) *Biochemistry 31*, 1695−1700.
Evans, P. R., & Hudson, P. J. (1979) *Nature (London) 279*, 500−504.
Evans, P. R., Farrants, G. W., & Hudson, P. J. (1981) *Philos. Trans. R. Soc. London, Ser. B 293*, 53−62.
Gratton, E., Alcala, J. R., & Marriott, G. (1986) *Biochem. Soc. Trans. 14*, 835−838.

Hill, A. V. (1910) *J. Physiol. London 40*, iv−vii.
Johnson, J. L., & Reinhart, G. D. (1992) *Biochemistry 31*, 11510−11518.
Johnson, J. L., & Reinhart, G. D. (1994a) *Biochemistry 33*, 2635−2643.
Johnson, J. L., & Reinhart, G. D. (1994b) *Biochemistry 33*, 2644−2650.
Kotlarz, D., & Buc, H. (1977) *Biochem. Biophys. Acta 484*, 35−48.
Kotlarz, D., & Buc, H. (1982) *Methods Enzymol. 90*, 60−70.
Lakowicz, J. R. (1983) in *Principles of Fluorescence*, pp 44−45, Plenum, New York.
Lipari, G., & Szabo, A. (1980) *Biophys. J. 30*, 489−506.
Monod, J., Wyman, J. L., & Changeux, J. P. (1965) *J. Mol. Biol. 3*, 318−356.
Munro, I., Pecht, I., & Stryer, L. (1979) *Proc. Natl. Acad. Sci. U.S.A. 76*, 56−60.
Reinhart, G. D. (1983) *Arch. Biochem. Biophys. 225*, 389−401.
Reinhart, G. D. (1985) *Biochemistry 24*, 7166−7172.
Reinhart, G. D. (1988) *Biophys. Chem. 30*, 159−172.
Reinhart, G. D., & Hartleip, S. B. (1987) *Arch. Biochem. Biophys. 258*, 65−76.
Reinhart, G. D., & Hartleip, S. B. (1992) *Arch. Biochem. Biophys. 296*, 224−230.
Reinhart, G. D., Hartleip, S. B., & Symcox, M. M. (1989) *Proc. Natl. Acad. Sci. U.S.A. 86*, 4032−4036.
Rubin, M. M., & Changeux, J. P. (1966) *J. Mol. Biol. 21*, 265−274.
Rypniewski, W. R., & Evans, P. R. (1989) *J. Mol. Biol. 207*, 805−821.
Schirmer, T., & Evans, P. R. (1990) *Nature 343*, 140−145.
Shirakihara, Y., & Evans, P. R. (1988) *J. Mol. Biol. 204*, 973−994.
Smith, D. K., Krohn, R. I., Hermanson, G. T., Mallia, A. K., Gartner, F. H., Provenzano, M. D., Fujimoto, E. K., Goeke, N. M., Olson, B. J., & Klenk, B. C. (1985) *Anal. Biochem. 150*, 76−85.
Symcox, M. M., & Reinhart, G. D. (1992) *Anal. Biochem. 206*, 394−399.
Voet, D., & Voet, J. G. (1995) *Biochemistry*, 2nd ed., pp 473−474, John Wiley & Sons, Inc., New York.
Weber, G. (1952a) *Biochem. J. 51*, 145−155.
Weber, G. (1952b) *Biochem. J. 51*, 155−167.
Weber, G. (1972) *Biochemistry 11*, 864−878.
Weber, G. (1975) *Adv. Protein Chem. 29*, 1−83.
Zeng, R.-L., & Kemp, R. G. (1992) *J. Biol. Chem. 267*, 23640−23645.

BI970942P